1	Application of EIS for Quantitative Coating Quality Assessment During Salt Cabinet			
2	Testing of High-Durability Coatings			
3				
4	Marina Mrđa Lalić, 1,2* and Sanja Martinez ¹			
5	¹ University of Zagreb, Faculty of Chemical Engineering and Technology, Department of			
6	Electrochemistry, Savska cesta 16/I, 10000 Zagreb, Croatia			
7	² Koncar Power Transformers Ltd, A Joint Venture of Siemens and Koncar d.d., Josipa			
8	Mokrovica 12 , 10000 Zagreb, Croatia			
9	*Corresponding author: E-mail: marina.mrda@siemens.com			
10	Phone: +385 99 2951 416			
11	Abstract			
12				
13	The aim of the study was to exemplify the benefits of using electrochemical impedance			
14	spectroscopy (EIS) for quantification of coating quality during accelerated corrosion testing. The			
15	study included an innovative application of the commercial flexible gel electrodes in a two-			
16	electrode setup for following the impedance of the two high-durability offshore coating systems			
17	exposed to 1440 h of neutral salt spray (NSS) according to EN ISO 9227. The results were			
18	compared to those of the EIS measurements during 8000 h long exposure to a liquid electrolyte in			
19	a press-on cell according to the established EN ISO 16773 method. Complementary methods of			
20	differential scanning calorimetry, Fourier transform infrared spectroscopy and thermogravimetric			
21	analysis have been used for surface, interface and depth profiling of coating characteristics that			
22	were commented with respect to the EIS results.			
23	EIS has been found to give sound quantitative results for coating impedance and a good estimation			
24	of long term coating behaviour within the first 100 h of accelerated exposure. It can be considered			
25	a promising tool for the early detection of coating damage during weathering tests.			
26				
27	Keywords: durability of coatings; EIS; salt spray chamber; organic coatings degradation			
28				
29				
30				
31				

1. Introduction

At present, epoxy and polyurethane coatings are the predominant types of coatings used in the offshore industry. Since offshore construction coatings face outdoor exposure continuously throughout their service life, which includes high relative humidity, rain, a saline corrosive atmosphere and high UV radiation, their lifetime is shortened. The expected lifetime for an offshore construction is 20 years or more and high-performance coatings are required for this application to avoid excessive and expensive maintenance operations and the loss of revenue. An anticorrosive coating system usually consists of multiple layers of different coatings with different properties and purpose. A typical anticorrosive system for highly corrosive marine environments usually consists of a primer, one or several intermediate coats, and a top coat. The function of the primer is to protect the substrate from corrosion and to ensure good adhesion to the substrate. The function of the intermediate coat is to build up the thickness of the coating system and impede the transport of aggressive species to the substrate surface. The topcoat is exposed to the external environment and must provide the surface with the required colour and gloss. The overall system is characterized by high electrical resistance and low capacitance which may quickly and easily be quantitatively measured, especially, after the development of advanced EIS instruments having: pA current measurement range, high input impedance up to 1 $T\Omega$, variable gain amplifiers, variable filters input front-ends and a floating ground. ^{2,3}

Over the last few decades, electrochemical methods have found widespread use for characterization of anticorrosive coatings and have been commonly employed to assess the performance and durability of anticorrosive coatings in the laboratory. By making periodic EIS measurements during the exposure to the corrosive environment, the level of coating damage can be estimated. EIS is a non-destructive measurement that may be used to track the condition of a coated metal sample as it changes. Equivalent circuit models using passive electrical engineering and physics circuit elements have commonly been used to help interpret EIS studies of coating systems. Data analysis procedures need to use non-linear, complex least squares fitting algorithm program of these equivalent electrical circuits (EEC) models to the EIS data. EEC is commonly used to interpret EIS studies of coating systems, but in some cases, calculated data from EEC models are not completely comparable with experimental data, moreover finding an exact matched model is quite difficult. The performance of the coating is evaluated according to the magnitude of

the parameters in the equivalent circuit and their changes with exposure time. $^{7\text{-}10}$ Other approaches such as minimum phase angle and its frequency, frequency breakpoint, the impedance at low frequency, the changing rate of impedance and phase angle at high frequencies have been used by some researchers to avoid these problems. 11 It is accepted among researchers that the initial step in the degradation process is the loss of dielectric properties of the polymer resulting from water ingress into the coating film. The relation between the initial and final coating capacitance may be an appropriate parameter by which to rank coating lifetime. 12 Also, low frequency coating resistance is taken as an indicator of coating quality. $^{7\text{-}9}$ Excellent coatings have resistance values 10^8 - 10^{12} Ω cm² and poor corrosion protection properties are exhibited when resistance intensity drops below 10^5 Ω cm2. 13 The appearance of coating defects is observed when coating impedance value falls below 10^6 Ω cm². 14 Impedance greater or equal to 10^9 Ω corresponds to excellent protecting properties of coatings which provide almost purely capacitive behaviour over long exposure periods. 15

The coatings industry also applies spectroscopic and thermal analysis methods that allow the assessment of coating characteristics before and after their exposure to a wide variety of service conditions. Fourier transform infrared (FTIR) spectroscopy is of non-destructive nature and it is used for the rapid detection of ageing processes and the wear of material and coatings, as well as for determining the interaction between substrate and coatings. This technique is used to provide the information of chemical structure characteristics of the coatings on metals. ¹⁶ With this method, the performance of coating systems can be estimated in a short test period. ¹⁷ The most important of these techniques include attenuated total reflectance (ATR). In this technique, the sample is placed in contact with the surface of an IR radiation absorbing material with a high refraction index (ATR crystal) and can be considered a surface analysis. A part of the radiation beam penetrates the sample and one part is reflected from the upper layers of coatings. ¹⁸ A significant limitation of this technique is that it needs excellent contact between the sample and the ATR crystal since deficient contacts drastically decrease the signal-to-noise relation and consequently the quality of the IR spectra obtained. This method has a significant disadvantage in the case of heterogeneous surfaces, as it happens with many coatings. Also, weakly transparent and highly pigmented coatings are hardly analysed by this technique. 19,20 In the study of corrosion protection of polymer coatings, insitu AFM measurement enables direct and real time monitoring of the change of surface layer.²¹

To obtain the information about the chemical and physical modification of the whole coating volume, the measurement of the glass transition temperature (Tg) using differential scanning calorimetry (DSC) can be useful. 18 Below Tg, the polymer chains of amorphous polymers are frozen into place by structural and kinetic effects to yield a rigid glassy state that drastically affects the mechanical, electrical, and transport properties of the polymers. Above Tg, the polymer goes into a rubbery state with an increase in molecular mobility and free volume. The transport properties of polymer-based coatings undergo a sharp increase at Tg, including the diffusion of permeants and coating conductivity. The last two specific transport properties are of much interest in the studies of the corrosion protective properties of organic coatings and their durability under conditions of use. The ingress of corrosive species must occur through the coating and along the metal/coating interface. Modifying chemical bonds causes changes in the polymer matrix Tg value during long-term exposure to poor atmospheric conditions. TGA is used for determining thermal and oxidative stability of materials as well as for compositional analysis of different materials and it is an excellent complement to the DSC method. 23

EIS is a very sensitive method that can generate quantitative data that relates to barrier properties of a coating on a metal substrate and can indicate changes in the coating long before any visible damage commences. Contrarily, a currently employed method to assess offshore coating quality relies on long-term cyclic exposure in a climatic chamber until visible signs of coating degradation appear. Moreover, the 2017 edition of EN ISO 12944-6 standard redefines coating durability classes and suggests the application of cyclic accelerated corrosion tests for C4 of high and very high durability and C5 coating systems of high and very high durability. Due to the long duration of 4200 h and a high cost of such tests, it is of great technical importance to investigate quantification of the coating quality by EIS with the prospects of early detection of coating degradation during accelerated testing as well as during exposure to service conditions.

In the present study, two coating systems consisting of zinc epoxy primer and two epoxy coats one with, and the other without the polyurethane topcoat, have been investigated. The focus of the investigation was on early detection of coating degradation during exposure to neutral salt spray (NSS) done according to the EN ISO 9227 standard and corresponding to the requirement for C5 and CX categories as defined by ISO 12944-6. EIS has been measured periodically during the NSS test by shortly stopping the exposure to salt mist and performing measurements with the flexible gel electrodes which enabled capturing of the momentary coating state.^{2,3,25-27} For comparison,

measurements have also been done by EIS according to EN ISO 16773 standard and by FTIR, DSC and TGA methods.

2. Experimental

2.1 Material and preparation

Carbon steel sheets with dimensions of (100 x 150 x 10 mm) were used as a metallic substrate. The samples were sand-blasted to Sa 2.5 (according to EN ISO 8501-1) and the surface was cleaned from visible oil and dirt. Two coating system denoted as System A and System B have been applied to the carbon steel panels by the air spraying technique. Specification of the selected coating systems is shown in Table 1. The minimum number of layers and the nominal film thickness of each coating is determined according to the type of coating materials, the corrosivity category and the required durability. System A corresponded to the System No. C5.7, for corrosivity category C5, with a lifetime of 15 to 25 years and a nominal dry film thickness (NDFT) > 260 μ m according to ISO 12944-5. System B corresponded to the System No. C5.8, for the extreme corrosivity category CX (Offshore) with a lifetime of range more than 25 years and an NDFT > 320 μ m. The coatings consisted of two components, a resin and a hardener component.

Table 1. Specifications for the investigated commercial coating systems

Coating	Number	Coating type	Cumulative	Base	Solid(s) %
system	of layers		thickness (μm)	polymer	by weight
System A	2	Basecoat	270	Zinc rich	50
		Intermediate coat		Epoxy	
System B	3	Basecoat	460	Zinc rich	36
		Intermediate coat		Epoxy	
		Topcoat		Polyurethane	

2.2. Instrumentation

2.2.1. Electrochemical impedance spectroscopy (EIS) measurements

EIS measurements started two months after the application of the coating which allowed for proper drying. EIS measurements were carried out at the open circuit potential (OCP) with a DC potential amplitude of 10 mV in the frequency range of 10⁴ Hz to 10⁻² Hz. The coated steel panels were put into a Faraday cage which eliminated external electromagnetic noise during the EIS testing. The three-electrode cell constructed according to EN ISO 16773 consists of an inert cylinder, which is attached to the coating surface and filled with electrolyte. A stainless-steel mesh serves as the counter electrode (CE) and the metal substrate is the working electrode (WE). The counter electrode has a circular hole in the middle where the calomel reference electrode (SCE) is protruding. 28 A two gel-electrode system consists of a pair low-cost, commercial polymeric gel electrodes placed in parallel at the surface of the metal.²⁹⁻³¹ One electrode is connected to the working electrode input of the potentiostat and the other to the reference and counter electrode input. Schematic setup of the measurement cells is shown in Figure 1. Details of the Recorr CQC customized instrumental setup that has been developed in our laboratory were presented previously.³² Calibration of the setup has been done according to EN ISO 16773-3, on a highimpedance dummy cell mimicking the coating. The EIS data is analysed based on the low frequency impedance at 0.1 Hz and the shape of the Bode plot curves. The performance of the coating is evaluated according to the magnitude of impedance and its change with the exposure time.33,8-9

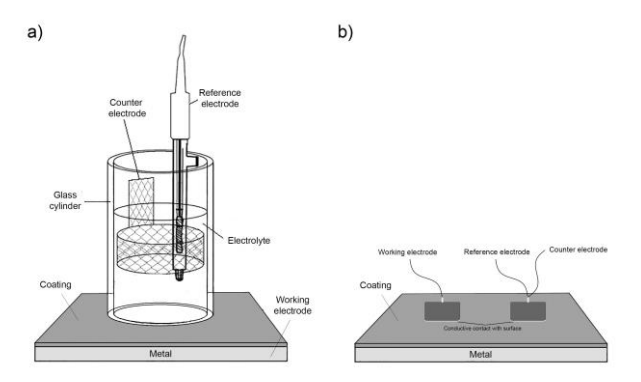


Figure 1. a) a three-electrode cell constructed according to EN ISO 16733 and b) a two-electrode setup.³²

For the three-electrode system the exposed coated sample area was 28,27 cm² and for the two-electrode system, the area was 32 cm². Coating degradation was induced in two ways: by exposure to liquid 3,5% sodium chloride (NaCl) at room temperature (21°C) for 8000 h in a test

147

148

149

150

151

152

153

154

155

156

157

158

159

160

161

162

163

164

165166

167

168

169

170

conducted according to EN ISO 16772 and by exposure to NSS of 5 % NaCl at 35°C according to EN ISO 9227 for 1440 h. In both cases measurements were carried out in time intervals that enabled capturing of the significant changes in the extent of coating degradation.

175

172

173

174

2.2.2. Fourier transform-infrared spectroscopy (FTIR) measurements

176177

178

179

180

181

182

183

184

185

186

187

188

189

190

191

192

193

194

195

196

197

Chemical changes were measured with attenuated Total Reflection - Fourier Transform Infrared (ATR - FTIR) spectroscopy method before and after exposure of the samples to external conditions. PerkinElmer spectrometer Spectrum One, USA connected to a computer program interface for capturing the sample spectrum has been used. The sample was placed in contact with a crystal of ATR, absorptive of the near infra-red radiation (IV) and of high refractive index, where part of the radiation penetrated in the sample and part was reflected.²⁰ The spectrum ranged from 400 to 4000 cm⁻¹ and each spectrum was an average of ten scans with a resolution of 4 cm⁻¹. This technique is highly sensitive to surface properties and conditions. High sensitivity to changes at the surface is particularly good for characterization of coating degradation due to weather conditions. The preferred format for presenting spectral data is transmittance format, which is the default output of most instruments and allows the best dynamic range for both weak and intense bands.³⁴ After scanning samples with the ATR - FTIR method, we prepared pellets of each coating systems and subjected them to FTIR measurements. The detector on ATR -FTIR has a limitation of the measurement range from 4000 to 650 cm⁻¹ and part of the spectrum between 650 and 200 cm⁻¹ is lost. Measurements of the pellets were therefore also done in a spectral range from 4000 to 350 cm⁻¹. 3 mg of scraped powder from the surface of each coated sample was mixed into 350 mg of spectroscopically pure KBr. The mixture was milled in agate mortar until we obtained a fine and very homogeneous mixture. Samples with KBr were then hydraulically pressed into a 13 mm stainless steel mold. The preparation of pellets was in accordance with the standard ASTM E1252:2007.³⁵

198

2.2.3. Thermogravimetric analysis (TGA) measurements

200201

202

199

Thermal stability of each coating system was investigated using Q500 (TA instruments) with auto sampler controlled by TA Universal Analysis software. The films were applied on a

plastic foil with an applicator in range 0.16 - 0.25 mm and dried at room temperature for 72 h. The experiments were performed in nitrogen atmosphere (flow of 40 - 60 ml min⁻¹) at a heating rate of $10 \, ^{\circ}$ C min⁻¹ over the temperature range of $1000 \, ^{\circ}$ C.

2.2.4. Differential scanning calorimetry (DSC)

DSC is a thermal analysis technique commonly used to determine parameters such as glass transition temperatures (Tg), melting points (mg) and heat capacities of materials. 9 Tg of samples was measured by DSC before and after exposure to the salt spray chamber. The measurements were carried out on Mettler Toledo DSC 823 controller at a scan rate of 20 °C min⁻¹ over the temperature range from 0 to 90°C in two heating cycles under a nitrogen atmosphere with a constant flow of 60 mL min⁻¹. All samples (10 mg \pm 3 mg) were weighed and sealed in a hermetic aluminium pan with lids. The measurement was conducted according to the EN ISO 11357.

3. Results and discussion

3.1. EIS Results

Measurements of impedance obtained by the two flexible electrodes setup are shown in Figure 2 for systems A and B. Bode plots of the intact coating show its excellent protective action, i.e. the low-frequency impedance greater than $1.0 \times 10^{11} \Omega$. Measurements of impedance obtained by the three electrodes setup in a cell filled with 3.5% NaCl are shown in Figure 3. The initial measurements were done after 2.5 h of exposure and the measured Bode curves show the low-frequency impedance value is already below $1.0 \times 10^{10} \Omega$, which is significantly lower than the impedance of the intact coating.

Low-frequency impedance read at 0.1 Hz and normalized by the electrode area is shown as a function of exposure time for coating systems A and B in Figure 3, for the NSS and 3.5% NaCl tests. It is evident that the low-frequency impedance value in all cases drops sharply during the first 100 h of exposure. For system A, in both tests, the final impedance falls to the values around $10^7 \, \Omega \, \text{cm}^2$, although initially being by almost an order of magnitude lower for the NSS test. This would imply that more severe corrosive conditions are attained during the NSS test than during immersion in 3.5 % NaCl when it comes to epoxy coating. Deflorian et al. compared the results obtained by

EIS and salt spray, have visually observed that the samples were nearly intact after more than three months of immersion but had many blisters on the coating after only a few weeks of salt spray exposure.³⁶

System A is made up of zinc rich basecoat and an epoxy topcoat applied at a thickness of 270 μ m. Hence, the drop in low-frequency impedance is larger for system A than for the System B that has an extra layer of polyurethane and a total thickness of 460 μ m.

For system B, in both tests, the final impedance falls to values around $10^{10} \,\Omega$ cm², although initially being by about half an order of magnitude higher for the NSS test. This would imply that more severe corrosive conditions are attained during the 3.5 % NaCl immersion test than during the NSS test when it comes to polyurethane coating. This is in concordance with the well-known, superior performance of epoxy coatings over the polyurethane coatings under immersion conditions.¹⁴

The oscillatory behaviour of impedance during the EIS tests has been observed previously and might be explained by pore blockage by corrosion products and the random formation of macroscopic perforations in the coating.³⁷ Although the authors refer to the observed oscillations as a drawback of the EIS method and its failure to give reproducible results, it should be noted that the result in fact shows the ability of EIS to authentically reflect the true state of the coating. The oscillatory effect is more pronounced for the lower quality coating and for the NSS exposure. Nevertheless, the average impedance of each system can readily be deduced from the plots and rating of the coating quality can be done with reasonable confidence. According to the literature criteria based on the impedance at 0.1 Hz,³⁸ system B may be rated as excellent and system A as fair.

Besides the quantitative rating of the coating quality, much can also be deduced from the shape of the Bode plots.³⁹ Fitting of the results to equivalent circuits is not considered in the present study because: (i) fitting is unreliable or even impossible for data recorded down to the frequency of only 10^{-2} Hz, that is usually set in order to quicken the measurements and (ii) fitting is questionable if done by the laboratory personal unacquainted with EIS. To simplify conclusions and explicate the potential for widespread use of the suggested method, the shape of the Bode curves is explained.

It is widely accepted that the EIS spectrum of an efficient protective coating can be presented by a simple model of capacitance in a parallel to a resistance.⁴⁰ High-frequency impedance response for the intact coating is a straight line with the unit negative slope and the phase angle close to -

90°, as seen from Figure 2 a) and Figure 3 a). Such a dependency is characteristic of almost pure capacitive behaviour. It is well known that, during exposure to an electrolyte, the coating first shows deviation from the capacitive behaviour. An increase of the phase angle slope from -1 to higher values in the high-frequency region signifies frequency dispersion that requires the substitution of pure capacitance for the CPE element in the coating equivalent circuit. CPE probably reflects water ingress within the polymer matrix causing a variety of RC combinations in parallel forming a distributed equivalent circuit.

Corrosion initiation at the substrate causes a second time constant appearance at frequencies below 1 Hz.⁴⁰ The low frequency response depends on the rate of the charge transfer reaction at the base of polymer defects and below the delaminated coating. The nested low-frequency equivalent circuit is comprised of a double layer capacitance and a polarization resistance. When diffusion effects in the coating pores are present, the Warburg element is added in series with the charge transfer resistance.

In the case of system A, the two time constant are clearly visible even for the 100 h of exposure to NSS. In the case of system B, a mild indication of the low-frequency time constant that almost completely overlaps with the high-frequency one is observed. Narrowing of the capacitive region, depression of the phase angle and deflection of the impedance slope from -1 are more pronounced for the system A.

For the 3.5% NaCl immersion tests, system A shows poorly resolved low-frequency time constant only for the longest time of exposure confirming the previously mentioned good protective properties of the epoxy coating under immersion conditions. System B again shows overlapping time constants but retains higher phase angle values than in the NSS experiment.

Photographs of both systems prior to exposure and after the NSS and 3,5% NaCl tests are shown in Figure 5. No apparent coating defects are visible. System B shows mild browning of the surface colour after the NSS test that may indicate substrate corrosion and corresponds to the pronounced low-frequency time constant observed for this coating. A conclusion about the comparable protective ability of the coatings might be drawn from the visual assessment of the coated specimen after the NSS and 3.5% NaCl tests. It is now obvious why the coating tests for high and very high durability coating systems given in the new edition of the EN ISO 12944-6 standard suggest gradual transfer from the NSS test to the considerably longer and more expensive

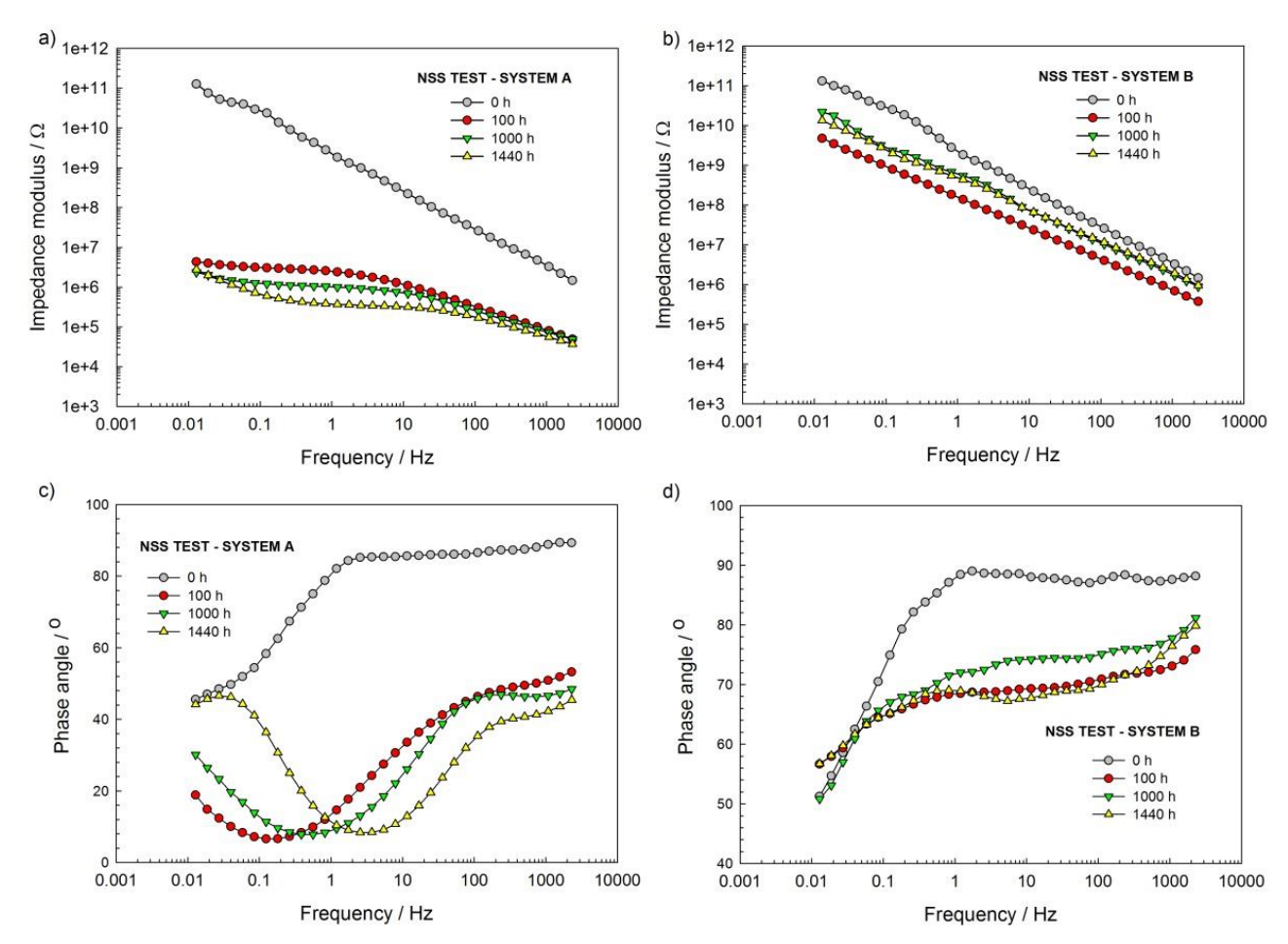


Figure 2. Bode plots of a) and c) system A samples and b) and d) of system B samples exposed to NSS according to EN ISO 9227 and measured by flexible electrodes in a two-electrode setup.

296

297298

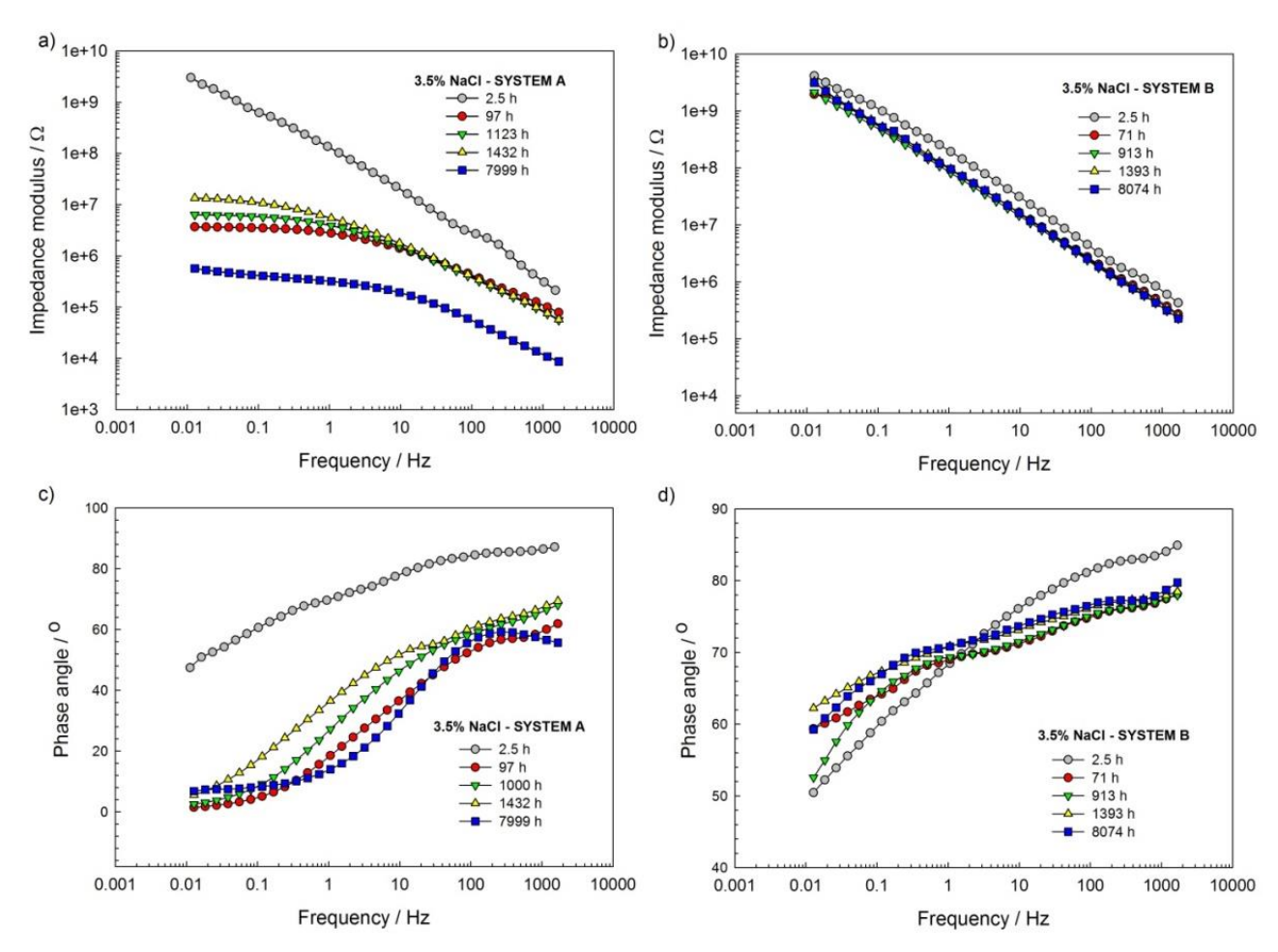


Figure 3. Bode plots of a) and c) system A samples and b) and d) of system B samples exposed to 3.5 % in a three-electrode cell constructed according to EN ISO 16733.

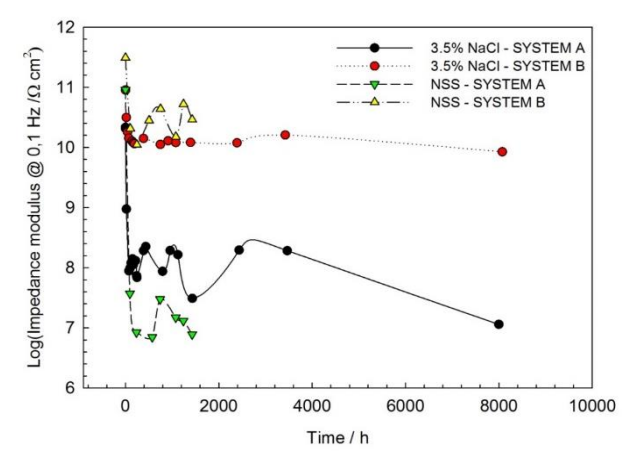


Figure 4. Low-frequency impedance read at 0.1 Hz as a function of exposure time for coating systems A and B during exposure to 3,5 % NaCl in the EN ISO 16773 test to NSS during the EN ISO 9227 test.

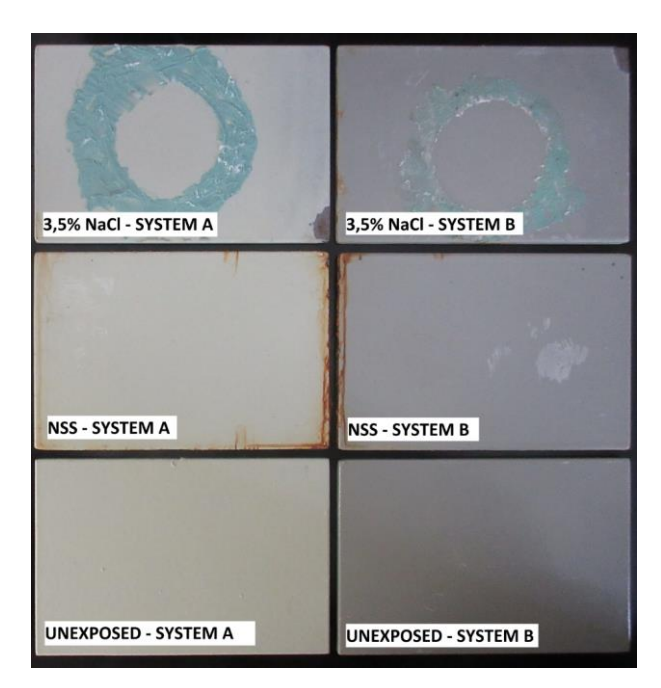


Figure 5. Photographs of specimens coating systems A and B before exposure, after exposure NSS and after exposure 3,5 wt% NaCl solution.

3.2. Characterization of coating system by FTIR

Figures 6 and 7 show the spectra for system A and B, respectively, before and after exposure to NSS and 3.5% NaCl tests. Spectra were obtained in two ways, by the ATR FTIR method and from KBr pellets containing scraped powder form the sample surface. It can be concluded that the spectrum shown in Figure 6 corresponds to epoxy resin bisphenol A with specific peaks at 827 cm⁻¹; 1245 cm⁻¹; 1509 cm⁻¹.⁴³ The spectra in Figure 7 correspond to polyurethane resin.⁴⁴

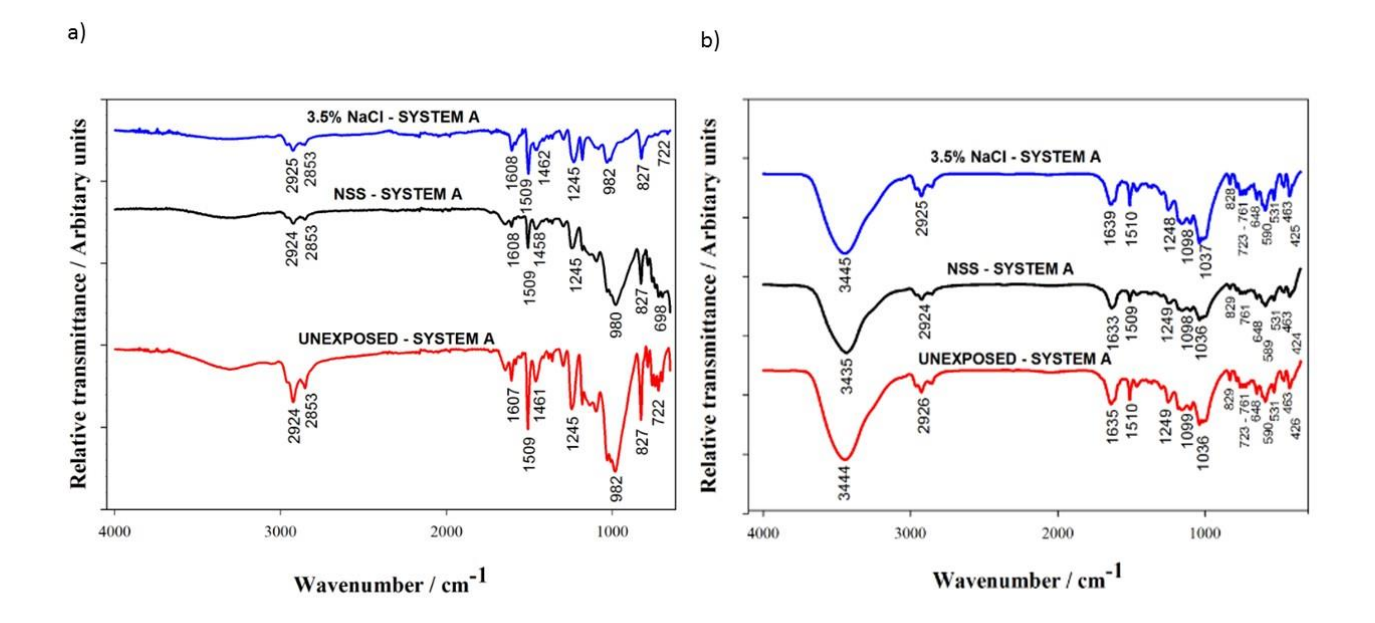


Figure 6. Spectra for system A before and after exposure to NSS and 3.5% NaCl tests obtained a) by the ATR FTIR method and b) from KBr pellets containing the scraped powder form the sample surface.

No clear conclusion about the difference in the state of the coatings before and after exposure can be deduced from the fingerprint region in Figures 6 and 7. The locations, the width and the intensity of the peaks of the investigated organic coatings do not change significantly after exposure which demonstrates a lack of degradation. No peaks corresponding to corrosion products are observed. New absorption peaks did not appear, except in the case of the system B exposed to 3.5% NaCl which shows a new peak at 2345 cm⁻¹ corresponding to CO₂.⁴⁵

It has been observed that when chemical bonds in the polyurethane coating are fractured under UV irradiation free radicals are generated, releasing CO₂.⁴⁵ Since the sample has not been exposed to UV irradiation, the appearance of CO₂ is probably due to the reaction of unreacted isocyanate with the water from the salt cabinet. The fact that CO₂ is observed only in the scraped powder indicates its residence within the polymer matrix.

S. Rashtchi et al. state that the spectral region between 3400 cm⁻¹ and 3700 cm⁻¹ is the best indicator of the moisture presence. 46 KBr pellets' peak at 3440 cm⁻¹ as well as the less resolved

peaks between 1634 and 1639 cm⁻¹ for both coating systems, denote the presence of water and indicate (-OH) stretching and scissors vibrations of the bonded water molecules, respectively. Higher absorption of moisture may be seen in the case of KBr pellets than in the case of ATR method because KBr easily absorbs water. Contrarily, ATR-FTIR measurements indicate a small amount of water in all the samples. It should be noted that after the NSS and 3.5% NaCl experiments the samples were left for 3 months at room temperature and humidity, which allowed them to dry.⁴⁷

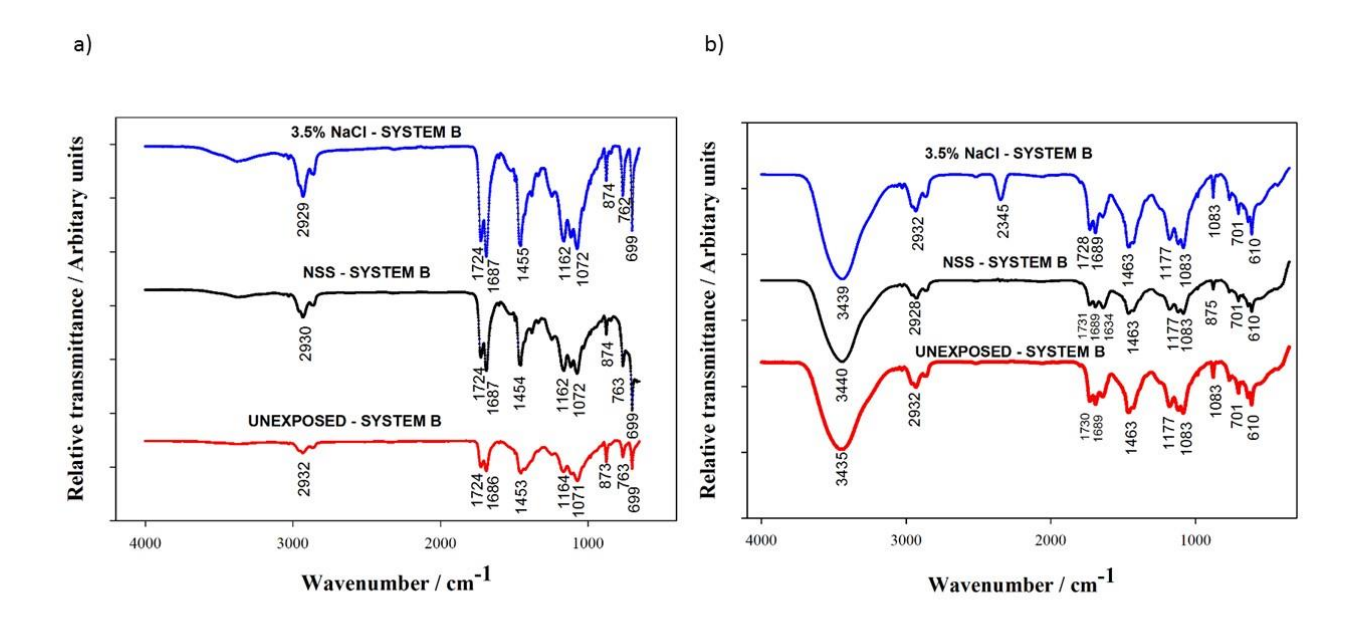


Figure 7. Spectra for system B before and after exposure to NSS and 3.5% NaCl tests obtained a) by the ATR FTIR method and b) from KBr pellets containing the scraped powder form the sample surface.

3.3. Characterization of coating system by DSC and TGA

Glass transition temperature for coating systems A and B before and after exposure to NSS in the EN ISO 9227 test and to 3,5 % NaCl in the EN ISO 16773 test is presented in Figure 8. Two glass transition temperatures denoted as T_{ghi} and T_{glo} have been measured for all the coatings indicating a biphasic system that could be related to the homogeneity of water distribution in the polymer.⁴⁸

For system A no significant change before and after exposure could be observed. The difference in T_g prior and after exposure barely exceeds the measurements uncertainty of DSC that may be taken as equal to 3 °C. DSC experiments were done on the same samples as FTIR. Apparently, after the 3 months drying period, the final state of the System A samples closely resembled the initial state showing that no irreversible changes have occurred within the polymer.⁴⁷

In the case of System B, a slight negative change is observed for T_{ghi} after the 3.5% NaCl test along with a moderate increase of all the other T_g . The increase in T_g value may be explained by the water ingress into the polymer network and secondary cross-linking through formation of multiple hydrogen bonds between water and polymer.⁴⁹

 T_{glo} is probably related to the water residing in the polymer free volume initially and after exposure and subsequent drying. The difference in T_g between the phases of about 20 °C is consistent with this assumption. According to Del Grosso the water in the intact coating can be detected with TGA at 110 °C. TGA curves of the intact epoxy and polyurethane coatings are shown in Figure 8 b. A weight losses of 1.62% for epoxy and 1.30%, for polyurethane, corresponding to the water content were recorded when temperature reached 1100 °C.

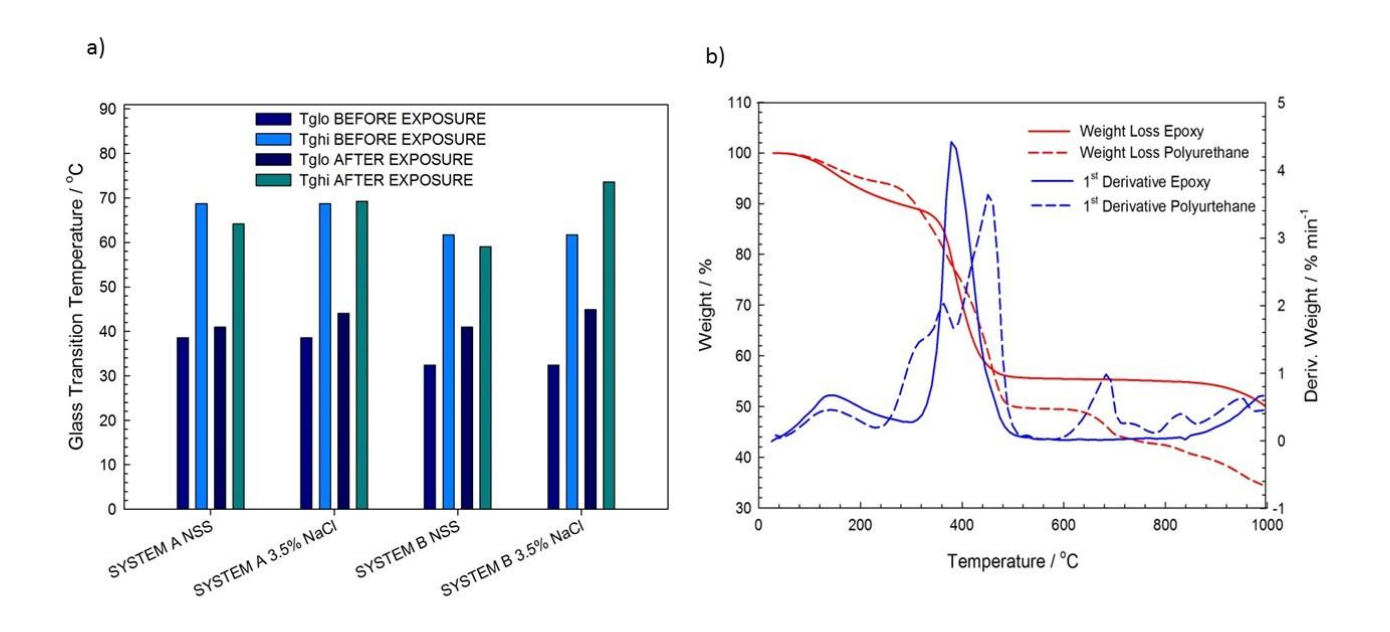


Figure 8. a) glass transition temperatures for coating systems A and B before and after exposure to NSS in the EN ISO 9227 test and to 3,5 % NaCl in the EN ISO 16773 test and b) TGA curves of intact epoxy and polyurethane coatings.

Full degradation occurred beyond 900°C leaving the residues of various weight loss percentages at the end of the TGA curve presented in Table 2. These are in good agreement with the declared percentage of solids by weight for the two coatings. TGA experiments showed two stages of weight loss for epoxy and three stages for polyurethane. An abrupt weight loss in coating systems was observed at high temperatures from approximately 300 to 500°C.

Table 2. Residual weight loss percentage of coating systems by thermogravimetric analysis

Coating system	Residue at 900 °C
System A	50,11
System B	34,29

4. Conclusions

It has been demonstrated by this investigation that the EIS method gives a possibility of quantification of coating degradation and estimation of its long-term performance from the first 100 h of exposure to NSS in the EN ISO 9227 test and to the 3.5% NaCl in EN ISO 16773 test. Contrarily, prolongation of the tests to 1440 h in the case of NSS exposure and to 8000 h in the case of 3.5 % NaCl exposure has produced no visible degradation signs on the coatings.

FTIR, DSC and TGA results preferentially gave information about the water absorbed within the coating that resides within the polymer free volume and within the polymer network. It has been shown that the coating polymer structure could almost completely reversibly return to the initial state after the experiments. Irreversible changes related to the degradation of barrier properties of the coatings, such as those related to the corrosion at the bottom of the coating pores and under delaminated coating are only detectible by EIS.

Finally, both, quantitation of the coating behaviour during long-term accelerated weathering exposures by the impedance modulus at 0.1 Hz and the analysis of the shape of the Bode plots can give early information about the coating quality. Widespread use of this method could reveal patterns common to the frequently used high-performance coatings, strengthen the conclusions of this study and considerably shorten the time and cost of coating quality assurance.

- 403 Acknowledgements:
- The authors would like to thank professor dr. sc. Mirela Leskovac from the Department of Surface
- Engineering of Polymer Materials, Faculty of Chemical Engineering and Technology to helped in
- 406 handling of the instruments for DSC and TGA methods and Ivana Šoić for help with FTIR method.

4. References

- 1. H. L. Dedeurwearder, Protecting Offshore Wind Farm Towers, *JPCL*, **2015**, https://www.paintsquare.com (assessed: March 04, 2019)
- 2. S. Grassini, S. Corbellini, M. Parvis, E. Angelini, F. Zucchi, *J. Int. Meas. Confed.*, **2018**, *114*, 508-514. **DOI:**10.1016/j.measurement.2016.07.014
- B. Ramirez Barat, E. Cano, Chem. Electro. Chem., 2018, 5, 2698-2716.
 DOI:10.1002/celc.201800844
- 4. P. A. Sørensen, S. Kiil, K. Dam-Johansen, C. E. Weinell, *J. Coat. Technol. Res.*, **2009**, *6*,135-176. **DOI:**10.1007/s11998-008-9144-2
- 5. D. Loveday, P. Peterson, B. Rodgers, Evaluation of Organic Coatings with Electrochemical Impedance Spectroscopy Part 2: Application of EIS to Coatings, http://www.consultrsr.net/files/jct/JCT200502.pdf (assessed: February 28, 2019)
- B. R. Hinderliter, S. G. Croll, D. E. Tallman, Q. Su, G. P. Bierwagen, *Electrochem. Acta*, 2006, 51, 4505-4515. DOI:10.1016/j.electacta.2005.12.047
- A. A. Hashem, J. A. Carew, A. Hasan, Surf. Coat. Int., 1999, 82, 26-30.
 DOI:10.1007/BF02693014
- 8. C. H. Tsai, F. Mansfeld, Corros. Sci., 1993, 49, 726-737. DOI:10.5006/1.3316106
- 9. C. Kong, *Material Mind.*, **2015**, 9, 27-28.
- S. Skale, V. Doleček, M. Slemnik, *Prog. Org. Coat.*, **2008**, *62*, 387-392.
 DOI:10.1016/j.porgcoat.2008.02.003
- 11. E. Akbarinezhad, M. Bahremandi, H. R. Faridi, F. Razaei, *Corros. Sci.*, **2009**, *51*, 356-364. **DOI:**10.1016/j.corsci.2008.10.029
- 12. L. De Rosa, T. Monetta, D. B. Mitton, F. Bellucci, *J. Electrochem. Soc.*, **1998**, *145*, 3830-3838. **DOI:**10.1149/1.1838881
- 13. J. Neshati, M. Faradi, Surf. Eng., 2009, 20, 299-303. DOI:10.1179/026708404225016418

- 14. S, Shreepathi, A. K. Gui, S. M. Naik, M. R. Vattipalli, *Jour. Coat. Techn. & Rese.*, **2011**, 8, 191-200. **DOI:**10.1007/s11998-010-9299-5
- 15. B. J. Merten, A. Skaja, D. Tordonato, D. Little, Re- evaluating Electrochemical Impedance Spectroscopy (EIS) for the Field Inspector's Tolbox: A Frst Approach https://www.usbr.gov/research/projects/researcher.cfm?id=2334 (assessed: February.28, 2019)
- J. T. Zhang, J. M. Hu, J. Q. Zhang, C. N. Cao, *Prog. Org. Coat.*, **2004**, *51*, 145-151.
 DOI:10.1016/j.porgcoat.2004.08.001
- X. F. Yang, C. Vang, D. E. Tallman, G. P. Bierwagen, S. G. Croll, S. Rohlik, *Polym. Degra. Stab.*, 2001, 74, 341-351. DOI: 10.1016/S0141-3910(01)00166-5
- F. Deflorian, L. Fedrizzi, S. Rossi, *Corros. Sci.*, **1998**, *54*, 98-605.
 DOI:10.5006/1.3287635
- 19. E. Almeida, M. Balmayore, T. Santos, *Prog. Org. Coat.*, **2002**, *44*, 233-242. **DOI:**10.1016/S0300-9440(02)00056-5
- 20. M. R. Costa, M. T. Santos, T C. Diamantino, Corros. Prot. Mater., 2011, 30, 57-64.
- 21. J. Li, L. Ecco, Fedel, Ermini, G. Delmas, J. Pan, *Prog. Org. Coat.*, **2015**, *87*, 179-188. **DOI:**10.1016/j.porgcoat.2015.06.003
- 22. J. Li, C. S. Jeffcoate, G. P. Bierwagen, D. J. Mills, D. E. Tallma, *Corros. Sci.*, **1998**, *54*, 763-771. **DOI:**10.5006/1.3284797
- 23. M. F. M. Nazeri, M. S. M. Suan, M. N. Masri, N. Alias, M. W. A. Rashid, Y. Alias, A. A. Mohamad, *Int. J. Electrochem.*, **2012**, *7*, 9633-9642.
- 24. J. Mlntyre, H. Pham, Prg. Org. Coat., 1996, 27, 201-207.
- 25. S. Grassini, Corros. Conser. Cult. Her Met. Art., 2013, 347-367.
 DOI:10.1533/9781782421573.4.347
- E. Anglini, S. Grassini, M. Parvis, F. Zucchi, Surf. Interface Anal., 2012, 44, 942-946.
 DOI:10.1002/sia.3842
- 27. S. Corbellini, M. Parvis, S. Grassini, *IEEE Transac. Instr. & Meas.*, 2012, 61,1193-1200.
 DOI:10.1109/TIM.2011.2175816
- 28. T. Bos, "Prediction of coating durability Early detection using electrochemical methods, *Delft University, The Netherlands, PhD Thesis,* **2008**.

- 29. S. Jamali, Y. Zhao, Z. Gao, H. Li, A. C. Hee, *J. Int. Eng. Chem.*, **2016**, *43*, 36-43. **DOI:**10.1016/j.jiec.2016.07.045
- 30. B. Ramirez Barat, E. Cano, P. Letardi, *Sens. Actuators B.*, **2016**, *43*, 36-43. **DOI:**10.1016/j.snb.2018.01.180
- **31**. Y. Kuo, Y. Lee, Y. L. Lee, *Jour. Inter. Measu. Confe.*, **2018**, *124*, 303-308. **DOI:**10.1016/j.measurement.2018.04.041
- 32. S. Martinez, Conference Corrosion and Surface Treatment in Industry, Viglas, Slovakia, 2019.
- **33**. A. A. Hashem, J. A. Carew, A. Hasan, *Surf. Coat. Int.*, **1999**, 82, 26-30. **DOI:**10.1007/BF02693014
- 34. J. Coates, Encyclopedia of Analytial Chemistry: Application, Theory and Instrumentation. Interpretation of Infrared Spectra A Practical Approach, Newtown, USA, **2006**.
- 35. "ASTM Standard E1252: General Techniques for Obtaining Infrared Spectra for Qualitative Analysis, *ASTM International*, **2007**.
- 36. F. Deflorian, S. Rossi, L. Fedrizzi, **2000**, 72, 81-87. **DOI:**10.1007/BF02698001
- 37. M. Del Grosso Destreri, J. Vogelsang, L. Fedrizzi, F. Deflorian, *Prog. Org. Coat.*, **1999**, *37*, 69-81. **DOI:**10.1016/S0300-9440(99)00056-9
- 38. L.Gray, B. Drader, M. O'Donoghue, R.Garret, J. Garret, R. Graham, V. Datta, *Corrosion NACE*, 2003, 03382.
- 39. A. Alizadeh Razin, B. Ramezanzadeh, H. Yari, *Prog. Org. Coat.*, **2016**, *92*, 95-109. **DOI:**10.1016/j.porgcoat.2015.11.023
- 40. F. Mansfeld, J. Appl. Electrochem., **1994**, 25, 187-202. **DOI:**10.1007/BF00262955
- 41. M. Kendig, J. Scully, *Corrosion*, **1990**, 46, 22-29. **DOI:**10.5006/1.3585061
- 42. G. M. Ferra, E. M. P. van Westing, J. H. W. de Wit, *Corrosion Sci.*, **1994**, *36*, 957-977. **DOI:**10.1016/0010-938X(94)90197-X
- 43. N. Tudorachi, F. Mustata, *Arab. J. Chem.*, **2017**. **DOI:**10.1016/j.arabjc.2017.07.008
- 44. E. A Papaj, D. J. Mills, S. S. Jamali, *Prog. Org. Coat.*, **2014**, *77*, 2086-2090. **DOI:**10.1016/j.porgcoat.2014.08.013
- 45. Y. Zhang, A spectroscopic study of the degradation of polyurethane coil coatings, *PhD Thesis*, *Queen Mary University of London*, **2012**.

- 46. S. Rashtchi, P. D. Ruiz, R. Wildman, I. Ashcroft, *SPIE Solar Energy and Technology*, San Diego, California, United States, **2012**. **DOI:**10.1117/12.928959
- 47. S. G. Croll, *Prog. Org. Coat.*, **2018**, *124*, 41-48. **DOI:**10.1016/j.porgcoat.2018.07.027
- 48. M. Y. M. Chiang, M. Fernandez-Garcia, *J. Appl. Polym. Sci.*, **2003**, 89, 1436-1444. **DOI:**10.1002/app.11576
- 49. N. Fredj, S. Cohendoz, X. Feaugas, S. Touzain, *Prog. Org. Coat.*, **2010**, *69*, 82-91. **DOI:**10.1016/j.porgcoat.2010.05.009
- F. Deflorian, S. Rossi, L. Fedrizzi, J. Coat. Teh., 2000, 72, 81-87.
 DOI:10.1007/BF02698001
- 51. M. Del Grosso Destreri, J. Vogelsang, L. Fedrizzi, F. Deflorian, *Prog. Org. Coat.*, **1999**, *37*, 57-67. **DOI:**10.1016/S0300-9440(99)00056-9